Proceedings of ES2009
Energy Sustainability 2009
July 19-23, 2009, San Francisco, California, USA

ES2009-90207

ANALYTICAL STUDY ON A VANED TYPE NOVEL AIR TURBINE FOR DIFFERENT CONDITIONS OF CASING AND ROTOR DIAMETERS

Bharat Raj Singh
Department of Mechanical Engineering,
Sagar Institute of Technology and Management,
Barabanki-225001, UP, India
Tel: +91-5248-220001 Mob: +91-9415025825
E-mail: brsinghlko@yahoo.com

Onkar Singh
Department of Mechanical Engineering,
Harcourt Butler Technological Institute, Nawabganj,
Kanpur-208002, UP, India
Tel: +91-512-2534001 Mob: +91-9415114011
E-Mail: onkpar@rediffmail.com

ABSTRACT

Greater utilization of hydrocarbon fuel in the transport sector is causing serious challenges to maintaining depletion of oil resources and also causing environmental and ecological imbalances. This makes it imperative to lay major thrust upon the search of alternative energy sources. Atmospheric air also offers one of the cost effective energy conversion system. The compressed air can be utilized as potential zero pollution working fluid for producing shaft work in the air turbine prime-mover for light vehicle. This paper details the mathematical modeling and performance evaluation of a small capacity compressed air driven vaned type novel air turbine. Effect of impingement and expansion action of high pressure air for different dimensional situations of casing and rotor diameters of the turbine have been considered and analyzed here. Study shows that the impingement work has significant contribution in total work output and varies from 2.4% to 16.8%, when other parameters like injection angle and vane angle are kept constant at 22.5^o and 36^o respectively and injection pressure varies from 2 to 6 bars,.

It is also concluded that the expansion work as well as total work is optimum when casing diameter (D) and rotor diameter (d) are 90 mm and 85 mm respectively.

Keywords: zero pollution, compressed air, air turbine, energy conversion, impingement action, injection angle

NOMENCLATURE

d	diameter of rotor (2r) in meter
D	diameter of outer (2R) cylinder in meter
F_{imp}	impingement force (Nfm)
L	length of rotor having vanes in meter
m	meter
n	no. of vanes=(360/θ)
N	no. of revolution per minute
p	pressure in bar
p_1, v_1	pressure and volume respectively at which air strike the Turbine,
p_4, v_4	pressure and volume respectively at which maximum expansion of air takes place,
p_5	pressure at which turbine releases the air to atmosphere.
r	radius of rotor (*d/2)* in meter
R	radius of outer casing (*D/2*) in meter
v	volume in cu-m
w	theoretical work output in Nm
W	theoretical power output (Nm/s)
X_{1i}	variable extended lengths of vane at point1
X_{2i}	variable extended lengths of vane at point 2
atm	atmospheric (1.0132 bar)
bar	(1 / 1.0132) atmospheric pressure
cu-m	cubic meter
HP	horse power
km	kilo-meter
kW	kilo-watt
min	minute
Nm	newton meter
psi	pound force per square inch (lbf/in^2)
rpm	revolution per minute

Subscripts

1, 2...4, 5	subscripts – indicates the positions of vanes in casing
i or imp	impingement
e or exp	expansion
t or total	total

Geek symbols

α angle BOF

α_1 angle LOF(=180-ϕ)

α_2 angle KOF(=180-θ-ϕ)

β angle BAF

γ 1.4 for air

θ angle between 2-vanes(BOH)

ϕ angle at which compressed air enters into rotor through nozzle

ξ_d eccentricity *(R-r)*

Δr_{mean} mean vane projection at injection pressure angle

1.0 INTRODUCTION

Worldwide consumption pattern of hydrocarbon fuel and its implications upon the environment and ecology are compelling to search for an environment friendly alternative to oil [1-9]. Ideally, such an alternative should have a zero or near zero pollution level, low initial cost, low running expenses, high degree of reliability, convenience and versatility of use. Use of compressed air for running prime mover like air turbine offers a potential solution to these issues, which does not involve combustion process for producing shaft work. Thus, the great advantages in terms of free of cost availability of air as fuel and the emissions free from hydrocarbons, carbon dioxide, carbon monoxide and nitrous oxides is apparent from such air motors. Compressed air driven prime movers are also found to be cost effective compared to fossil fuel driven engines. It only has perennial compressed air requirement which needs some source of energy for running compressor whose overall analysis shows that the compressed air system is quite attractive option for light vehicle applications [10].

Pioneering work in this area of compressed air engines has been done by French technologists Guy Negre and Saint Hilaire, G**.,** who developed air engine and quasi turbine respectively [11-12]. Numerous studies for optimizing efficiency of these air turbines have been done [13- 17].

The parametric analysis of a small capacity air turbine with vane type rotor has been carried out and presented in this paper. Results obtained using the mathematical modeling are presented and analyzed in light of various conditions of casing diameter (D) and rotor diameter (d). Forty five sets of readings were recorded. However, only twelve sets are shown in this paper at varying pressure of 2-6 bars (30-90 psi) and in the range of speeds 500-2500 rpm at constant vane angle 36^{o}and injection angle 22.5^o.

2.0 VANED TYPE NOVEL AIR TURBINE

In this study a vaned air turbine shown in Figure 1, has been considered. This air turbine is tested in order to get an output of 6.50 to 7.20 HP for meeting starting torque requirements at 500–750 rpm at 4-6 bar air pressure. The average running torque is available at normal speed of 2000–2200 rpm at 2-3 bars air pressure. The air turbine with single inlet and exhaust has spring loaded vanes to maintain regular contact with the elliptical bore. The various efforts have been made to get optimum shaft output produced [18-22].

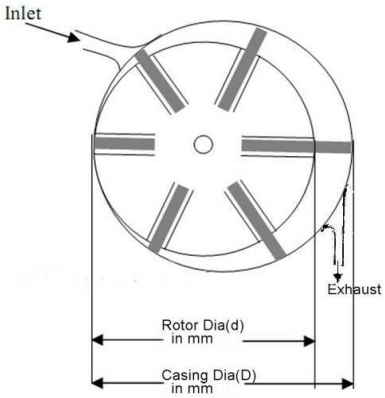

Figure 1: Air Turbine

3.0 MATHEMATICAL MODELING

The high pressure of air at ambient temperature drives the rotor in novel air turbine shown in Figure 1. When high pressure air enters through the inlet passage and impinges upon the vanes it produces impulse. Also the high pressure air entering the rotor in consecutive vanes is gradually expanded up to exit passage. This impingement action and the expansion of high pressure air both contribute in producing the shaft work from air turbine.

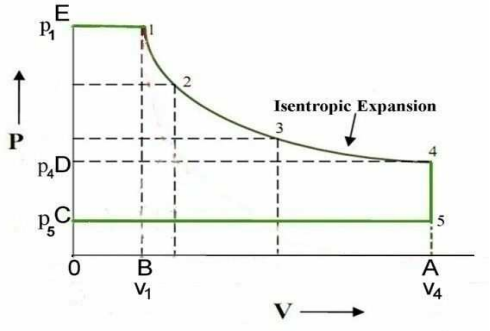

Figure 2: Thermodynamic Process (Isobaric, adiabatic and isochoric expansions)

Assuming isentropic expansion as shown in Figure 2, theoretical expansion work output would be:
Work done due to expansion cycle = Area under (E14DE) = Area under (E1BOE) + Area under (14AB1) – Area under (4AOD4).

$$workdone = (p_1v_1 - p_4v_4) + \left(\frac{p_1v_1 - p_4v_4}{\gamma - 1}\right)$$

$$= \left(\frac{\gamma}{\gamma - 1}\right)(p_1v_1 - p_4v_4)$$

Since for adiabatic expansion pv^{γ} = constant

$= p_1v_1^{\gamma} = p_4v_4^{\gamma}$, then $v_4 = \left(\frac{p_1}{p_4}\right)^{\frac{1}{\gamma}} v_1$

Applying these values above, then work done due to expansion can be written as

$$w_1 = \left(\frac{\gamma}{\gamma-1}\right).p_1.v_1.\left\{1-\left(\frac{p_4}{p_1}\right)^{\frac{\gamma-1}{\gamma}}\right\} \quad (1)$$

In this expansion process; pressure p_4 can't fall below atmospheric pressure p_5, thus at constant volume when pressure p_4 drops to exit pressure p_5, no physical work is seen. Since turbine is functioning as positive displacement machine and hence under steady fluid flow at the exit of the turbine, the potential work is absorbed by the rotor which may be written as,

$$w_2 = (\Delta w) = \int_4^5 v dp = (p_4 - p_5)v_4 \quad (2)$$

Thus net work done $'w'$ using equation (1) and (2),

$$w = (w_1 + w_2) = \left(\frac{\gamma}{\gamma-1}\right)p_1v_1\left\{1-\left(\frac{p_4}{p_1}\right)^{\frac{\gamma-1}{\gamma}}\right\} + (p_4 - p_5)v_4 \quad (3)$$

When air turbine is having "*n*" number of vanes, shaft output for one revolution shall be written as under: -

$$nw = n\left(\frac{\gamma}{\gamma-1}\right)p_1v_1\left\{1-\left(\frac{p_4}{p_1}\right)^{\frac{\gamma-1}{\gamma}}\right\} + n(p_4 - p_5)v_4 \quad (3a)$$

It is obvious from Figure 1, that if vanes are at angular spacing of θ degree, then total number of vanes would be, n = (360/θ).

The volumetric expansion from inlet to exit i.e. v_1 *to* v_4 can be derived by the variable extended length of vane as shown in Figure 3, at every point of movement between two consecutive vanes.

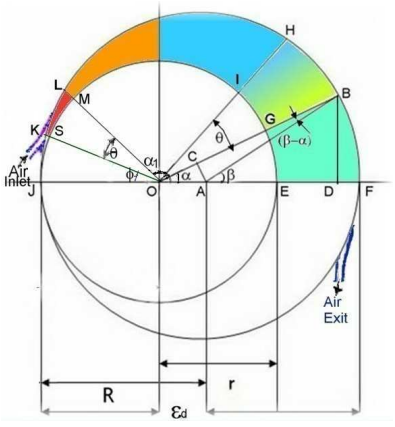

Figure 3: Variable length BG and IH and injection angle ϕ

From Figure 3, variable length BG would be,
BG= X at variable α

$$X_{variable} = R\cos\left[\sin^{-1}\left\{\left(\frac{R-r}{R}\right)\sin\alpha\right\}\right] + (R-r)\cos\alpha - r \quad (4)$$

and variable volume of cuboid (B-G-I-H-B):

$$v_{cuboid} = L\left\{\frac{(X_1 + X_2)(2r + X_1)}{4}\right\}\sin\theta \quad (5)$$

The volume at inlet v_1 or $v_{\min}$ will fall between angles
$\angle$LOF= $\alpha_1 = (180 - \theta - \phi)$ and
$\angle$KOF= $\alpha_2 = (\alpha_1 + \theta) = (180 - \phi)$,

when air is injected at angle ϕ into air turbine. Applying above conditions into equation (4), then

$$X_{1\min} = R\cos\left[\sin^{-1}\left\{\left(\frac{R-r}{R}\right)\sin(180-\theta-\phi)\right\}\right] + \left[(R-r)\cos(180-\theta-\phi) - r\right] \quad (6)$$

$$X_{2\min} = R\cos\left[\sin^{-1}\left\{\left(\frac{R-r}{R}\right)\sin(180-\phi)\right\}\right] + \left[(R-r)\cos(180-\phi) - r\right] \quad (7)$$

Applying values of X_{1min} and X_{2min} to equation (5), then volume at entrance v_1 or $v_{\min}$ will be

$$v_1 = L\left\{\frac{(X_{1\min} + X_{2\min})(2r + X_{1\min})}{4}\right\}\sin\theta \quad (8)$$

The volume at exit v_2 *or* $v_{\max}$ will fall between angles $\angle$BOF and $\angle$HOB, when OB touches OF [i.e. $\alpha = 0$ and $(\alpha + \theta) = \theta$]. It can be seen from Figure 3.

Applying above conditions into equation (4), then

$$X_{1\max} = 2(R - r) \Rightarrow (D - d) \quad (9)$$

$$X_{2\max} = R\cos\left[\sin^{-1}\left\{\left(\frac{R-r}{R}\right)\sin\theta\right\}\right] + \left\{(R-r)\cos\theta\right\} - r \quad (10)$$

Applying values of X_{1max} and $X_{2\,max}$ to equation (5), then volume at exit v_2 *or* $v_{\max}$ will be

$$v_2 = L\left\{\frac{(X_{1\max} + X_{2\max})(2r + X_{1\max})}{4}\right\}\sin\theta \quad (11)$$

Work output per unit time (power) from novel air turbine will be sum of both impingement action and expansion work

$$W_{total} = W_{exp} + W_{imp} \quad (12)$$

The expansion work W_{exp} in per unit time (Power) at speed of revolution (N) rpm, can be written as

$$W_{exp}=n(N/60)\left(\frac{\gamma}{\gamma-1}\right)\left\{1-\left(\frac{p_4}{p_1}\right)^{\frac{\gamma-1}{\gamma}}\right\}p_1\left[L\left\{\frac{(X_{1\min}+X_{2\min})(2r+X_{1\min})}{4}\right\}\sin\theta\right] \quad (13)$$
$$+n(N/60)(p_4-p_5)\left[L\left\{\frac{(X_{1\max}+X_{2\max})(2r+X_{1\max})}{4}\right\}\sin\theta\right]$$

The impingement work W_{imp} in per unit time (power) due to impact of nozzle air, can be written as

$$W_{imp} = (T \times \omega) \quad (14)$$

where torque $T=$ Force $\times$ Mean Projected length $= F_{imp}(r+\Delta r_{mean})$ (15)

and $$F_{imp} = p_1 a \quad (16)$$

Assuming p_1 = Pressure at which it strikes the vane
a = Area on which nozzle air pressure impinging

Substituting the value of equations (15) and (16) into equation (14),

$$W_{imp}=(T\omega)=2\pi(N/60)p_1L\left[\Delta r_{mean}(r+\Delta r_{mean})\right],$$

where $\Delta r_{mean}=\left(\frac{X_{1\min}+X_{2\min}}{2}\right)$

or $$W_{imp}=2\pi(N/60)p_1L\left(\frac{X_{1\min}+X_{2\min}}{2}\right)\left[r+\left(\frac{X_{1\min}+X_{2\min}}{2}\right)\right] \quad (17)$$

Substituting the values of W_{exp} from equation (13) and W_{imp} from equation (17) into equation (12),

The total shaft output of air turbine W_{total} in per unit time (power), can be written as,

$$W_{total}=n(N/60)\left(\frac{\gamma}{\gamma-1}\right)\left\{1-\left(\frac{p_4}{p_1}\right)^{\frac{\gamma-1}{\gamma}}\right\}p_1\left[L\left\{\frac{(X_{1\min}+X_{2\min})(2r+X_{1\min})}{4}\right\}\sin\theta\right] \quad (18)$$
$$+n(N/60)(p_4-p_5)\left[L\left\{\frac{(X_{1\max}+X_{2\max})(2r+X_{1\max})}{4}\right\}\sin\theta\right]$$
$$+2\pi(N/60)p_1L\left(\frac{X_{1\min}X_{2\min}}{2}\right)\left[r+\left(\frac{X_{1\min}+X_{2\min}}{2}\right)\right]$$

Table 1: Input Parameters

Symbols	Parameters
D=2R, d=2r	**Case *1*.** For Decreasing (D-d) for (D,d) values of (100, 80),
	Case *2*. For Constant (D-d) for (D, d) values of (100, 90), (90, 80), (80, 70), (70, 60), (60, 50), (50, 40), (45, 35).
	Case *3*. For Constant volume for (D, d) values of (100, 96), (90, 85), (80, 75), (70, 64), (60, 53), (50, 41), (45, 35).
p_1	30psi(≈2bar), 45 psi(≈3bar), 60 psi(≈4bar), 75 psi(≈5bar), 90 psi(≈6bar)
p_5	1 atm = 1.0132 bar
p_4	1.1 to 1.2 p_5 =1.1 bar
n	Number of vanes (360 / θ)
N	500 rpm, 1500 rpm, 2500 rpm
L	35mm length of rotor
γ	1.4 for air
θ	36^0 angle between 2-vanes, (i.e. rotor contains correspondingly 10 number of vanes)
ϕ	22.5^0 angle at which compressed air through nozzle enters into rotor

4.0 RESULTS AND DISCUSSION

Various input parameters considered for this study are listed in Table 1. Based on the mathematical model of air turbine, the effect of injection angles, speed of rotation and injection pressure to the expansion work in per unit time, impingement work in per unit time and total work output in per unit time are studied. Here the vane angle θ and injection angle ϕ of the air turbine is considered to be constant for whole study. The results obtained have been plotted towards following geometrical constraints:

Case 1

Power output as a function of casing and rotor diameters i.e. declining (D-d), for injection pressure 2-6 bars (30-90 psi) and rotational speed (500, 1500, 2500 rpm) and with vane angle 36^o and injection angle 22.5^o

From Figure 4, it is evident that the shaft work due to expansion power (W_{exp}) at 500 rpm is larger at 2 bars (30 psi) for (D-d) =20 mm and thereafter it gradually decreases at (D-d) =15 mm and 10mm. Also expansion power is seen to be higher for higher injection pressure 4 to 6 bars, which attributes to the large work capacity at higher injection pressures and reduces rapidly when (D-d) is kept 10 mm. Similar variations are also observed at higher speed 1500 rpm, 2500 rpm but expansion work is higher in comparison to 500 rpm.

From Figure 5, it is apparent from graphical patterns that the impingement work per unit time (W_{imp}) at 500 rpm is larger at 2 bars (30 psi) for (D-d) =20 mm and thereafter it gradually decreases at (D-d) =15 mm and 10mm. The shaft work in per unit time (power) due to impingement is small at low injection pressures and increases with increase in injection pressure. Higher impingement power at higher injection pressure is because of the large work potential of entering air stream. Similar variations are also observed at higher speed of rotations 1500 rpm, 2500 rpm but impingement power is higher in comparison to 500 rpm.

From Figure 6, it is observed that percentage contribution of expansion power at 500 rpm is lowest at 2 bar (30 psi), (D, d) = (100, 80) and almost constant at (D, d) = (90, 70). It increases at (D, d) = (80, 65) and almost constant at (D, d) = (70, 55) and (60, 45). It further increases at (D, d) = (50, 40) and almost constant at (45, 35). It signifies that the expansion power contribution is at minimum, when the (D, d) is (100, 80) and increases as D, d is lowered to (45, 35). At the same time for constant (D-d) contribution of expansion power is almost constant. At higher injection pressures of 3 to 6 bars (45 to 90 psi) the contribution of expansion power is lower at bigger diameters of (D,d) and increases as the casing , rotor diameters decreases (i.e. 45, 35 mm). The contribution of expansion power is found to follow same trend at different speeds of rotation 1500, 2500 rpm.

The contribution of impingement power is found to follow same trend at different speeds of rotation 1500, 2500 rpm (figures not shown here).

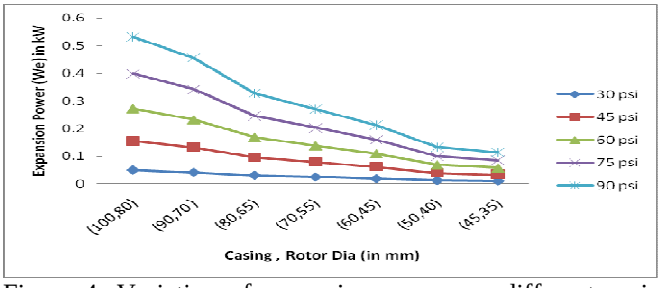

Figure 4: Variation of expansion power vs. different casing and rotor diameters at different air injection pressure at 500 rpm

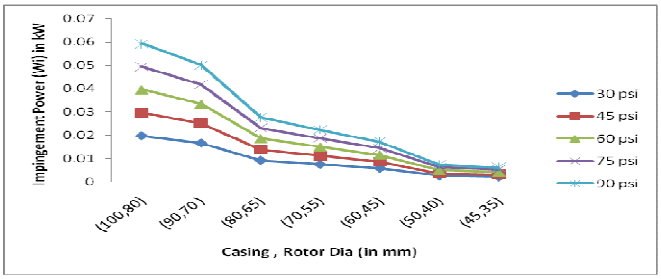

Figure 5: Variation of impingement power vs. different casing and rotor diameters at different air injection pressure at 500 rpm

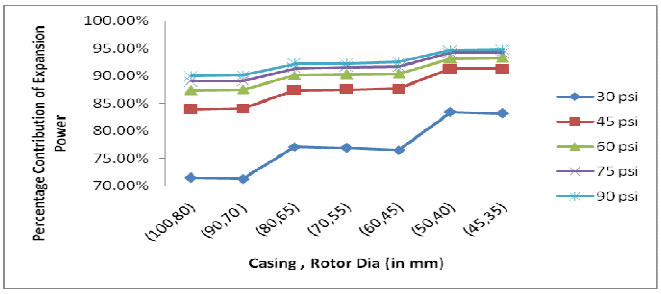

Figure 6: Percentage contribution of expansion power vs. different casing and rotor diameters at different air injection pressure at 500 rpm

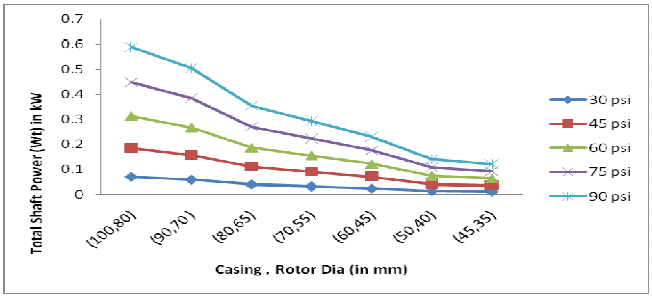

Figure 7: Variation of total power vs. different casing and rotor diameters at different air injection pressure at 500 rpm

Variation of total work output in per unit time is shown in Figure 7, for different air injection pressure (2 - 6 bars) and at 500 rpm. At 2 bar (30 psi) injection pressure total power (W_{total}) is seen larger when casing, rotor diameters and its difference are bigger. It gradually decreases when casing, rotor diameters and its difference are smaller. With increase in injection pressure (3 bar to 6 bar), the total power output increases gradually as shown in graphical patterns. Also total power output is more at higher speed of rotation

Case 2

Power output at different casing and rotor diameters when difference (D-d) remains constant for injection pressure 2-6 bar (30-90 psi) and rotational speed 500, 1500, 2500 rpm and with vane angle 36°and injection angle 22.5°

From Figure 8, it is evident that the shaft power due to expansion W_{exp} at 500 rpm and 2 bar (30 psi) is largest at (100, 90) mm casing, rotor diameters and thereafter gradually decreases linearly on decreasing casing, rotors diameters from (80, 70) to (45, 35) mm. Also expansion power is seen to be larger for higher injection pressure 4 bar to 6 bar, which is attributed to the large work capacity at injection pressures and reduces linearly to the casing, rotor diameter (45, 35) mm. Similar variations are also observed at higher speed 1500 rpm, 2500 rpm but expansion power is higher in comparison to 500 rpm.

From Figure 9, it is apparent from graphical patterns that the impingement power (W_{imp}) at 500 rpm and 2 bar (30 psi) is large at (100, 90) mm casing, rotor diameters and thereafter gradually decreases linearly on decreasing casing, rotors diameters from (90, 80) to (45, 35) mm. The shaft power due to impingement is small at low injection pressures and increases with increase in injection pressure. Higher impingement power at higher injection pressure is because of the large work potential of entering air stream. Similar variations are also observed at higher speed of rotations 1500 rpm, 2500 rpm but impingement power is higher in comparison to 500 rpm.

From Figure 10, it is observed that percentage contribution of expansion power at 500 rpm and 2 bar (30 psi) is small at (100, 90) mm casing, rotor diameters and almost constant on decreasing casing, rotors diameters from (90, 80) to (45, 35) mm. At higher injection pressures of 3 to 6 bars (45 to 90 psi) the contribution of expansion power is on further increasing side. The contribution of expansion power is found

to follow same trend at different speeds of rotation 1500, 2500 rpm.

The percentage contribution of impingement power is found to follow same trend at different speeds of rotation 1500, 2500 rpm (figures not shown here).

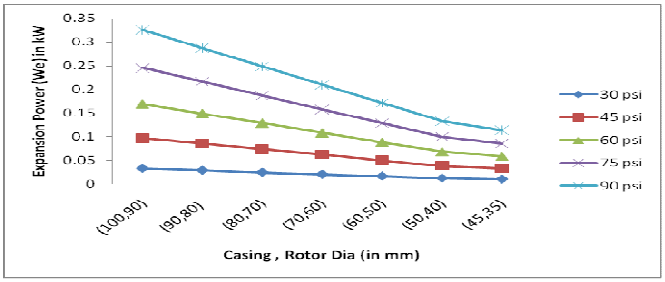

Figure 8: Variation of expansion power vs. different casing and rotor diameters when (D-d) is kept constant and at different air injection pressure at 500 rpm

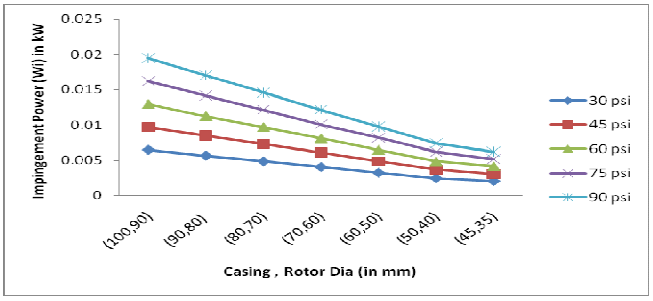

Figure 9: Variation of impingement power vs. different casing and rotor diameters when (D-d) is kept constant and at different air injection pressure at 500 rpm

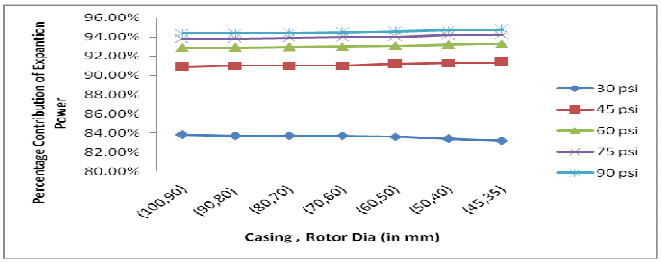

Figure 10: Percentage contribution of expansion power vs. casing and rotor diameters when (D-d) is kept constant and at different air injection pressure at 500 rpm

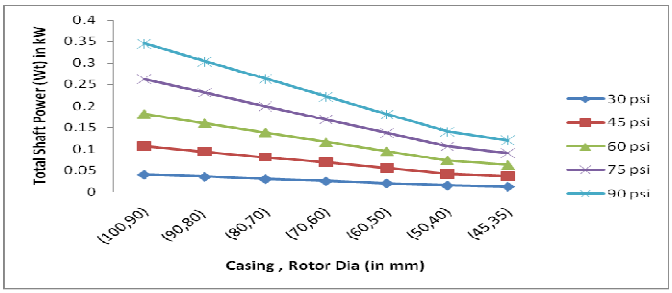

Figure 11: Variation of total power vs. different casing and rotor diameters when (D-d) is kept constant and at different air injection pressure at 500 rpm

Variation of total power output is shown in Figure 11, for different air injection pressure (2 - 6 bars) and at speed of rotation 500 rpm. Total power (W_{total}) at 2 bars (30 psi) is seen larger at (100, 90) mm casing, rotor diameters and gradually decreases on decreasing casing and rotor diameters from (90, 80) to (45, 35) mm. With increase in injection pressure (3 bar to 6 bar), the total work power increases gradually as shown in graphical patterns. Also total power output is more at higher speed of rotation.

Case 3

Power output at constant volume between casing and rotor diameters, for injection pressure 2-6 bar (30-90 psi) and rotational speed 500, 1500, 2500 rpm and with vane angle 36^o and injection angle 22.5^o

From Figure 12, it is evident that the shaft power due to expansion (W_{exp}) at 500rpm and 2 bar (30 psi) is small for (100, 96) mm casing, rotor diameters, suddenly it becomes largest at (90, 85) mm and thereafter drops down at (80, 75), it gradually decreases at casing, rotors diameters from (70, 64) mm to (45, 35) mm. Also expansion power is seen to be larger for higher injection pressure 4 to 6 bars, which is attributed to the large work capacity as injection pressures increases but it is optimum at casing, rotor diameters (90, 85) mm in all situations. Similar variations are also observed at higher speed 1500 rpm, 2500 rpm but expansion power is higher in comparison to 500 rpm.

From Figure 13, it is apparent from graphical patterns that the impingement power (W_{imp}) at 500 rpm and 2 bar (30 psi) is small for casing, rotors diameters (100, 96) mm, suddenly it becomes highest at (90, 85) mm, drops down at (80, 75) mm and thereafter it gradually increases at casing, rotors diameters from (70, 64) mm to (45, 35) mm. The shaft power due to impingement is small at low injection pressures and increases with increase in injection pressure. Higher impingement power at higher injection pressure is because of the large work potential of entering air stream. Similar variations are also observed at higher speed of rotations 1500 rpm, 2500 rpm but impingement power is higher in comparison to 500 rpm.

From Figure 14, it is observed that percentage contribution of expansion power at 500 rpm and 2 bar (30 psi) is large at casing, rotor diameters (100, 96) mm, drops down at (90, 85) mm and gradually declines from (70, 64) mm to (45, 35) mm. At higher injection pressures of 3 to 6 bars (45 to 90 psi) the contribution of expansion power is larger and follows the same trend from (100, 96) mm to (45, 35) mm as explained for injection pressure 2 bar (30 psi). The contribution of expansion power is also found to follow same trend at different speeds of rotation 1500, 2500 rpm.

The percentage contribution of impingement power is also found to follow same trend at different speeds of rotation 1500, 2500 rpm (figures not shown).

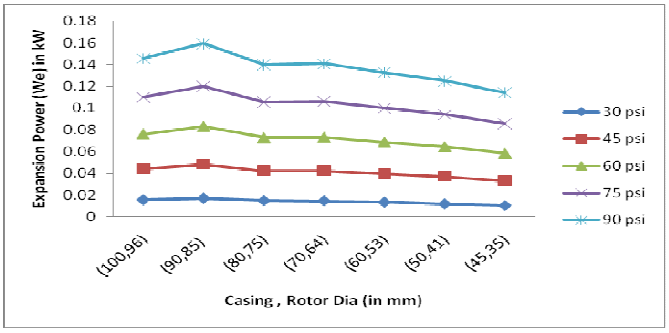

Figure 12: Variation of expansion power vs. different casing and rotor diameters when Volume is kept constant and at different air injection pressure at 500 rpm

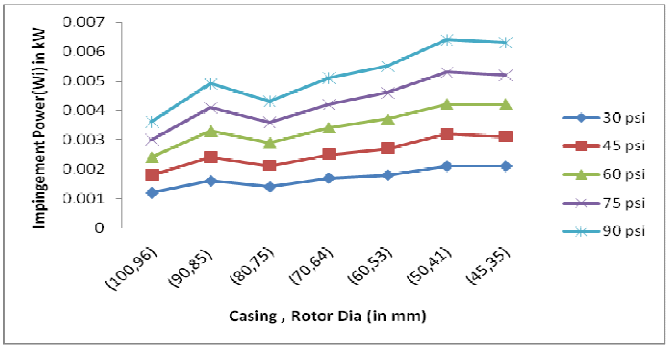

Figure 13: Variation of impingement power vs. different casing and rotor diameters when volume is kept constant and at different air injection pressure at 500 rpm

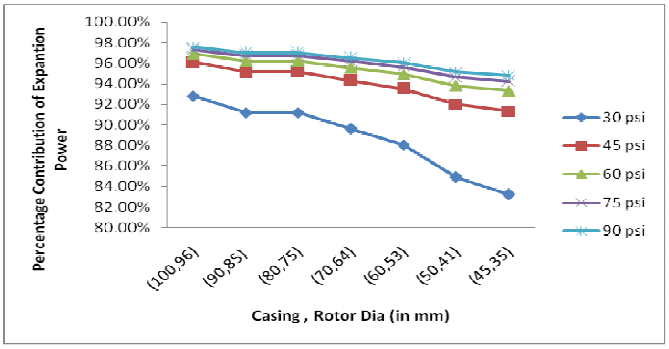

Figure 14: Percentage contribution of expansion power vs. different casing and rotor diameters when volume is kept constant and at different air injection pressure at 500 rpm

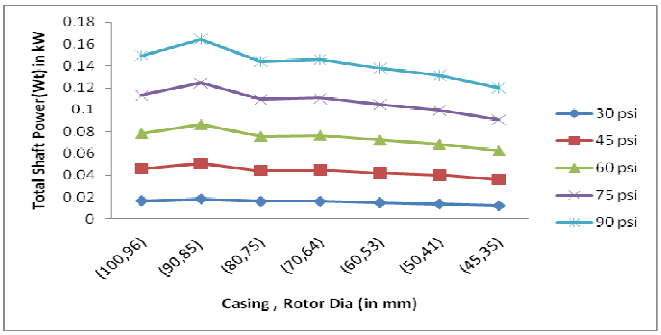

Figure 15: Variation of total power output vs. different casing and rotor diameters when volume is kept constant and at different air injection pressure at 500 rpm

Variation of total power output from air turbine with respect to constant volume between different casing and rotor diameters and at 500 rpm speed is shown in Figure 15. It is small for (100, 96) mm casing, rotor diameters, suddenly it becomes largest at (90, 85) mm and thereafter drops down at (80, 75), it gradually decreases at casing, rotor diameters from (70, 64) mm to (45, 35) mm. but it is optimum at casing, rotor diameters (90, 85) mm in all situations. Also total power output is more at higher speed of rotation 1500 rpm, 2500 rpm.

It is, therefore, observed that in the vane turbine total power output is combined effect of the component of impingement and expansion. Impingement also has significant contribution in total shaft output and varies for *Case 1*, 16.7% to 5.2% for declining (D-d) from 20 to 10 mm, Case 2, 16.8% to 5.2% for constant (D-d) as 10 mm and *Case 3*, 16.7% to 2.4% for constant volume between D and d, at varying injection pressures 2 to 6 bar, constant injection angle 22.5° and constant vane angle 36°. Thus it is also concluded that the expansion power as well as total power output is optimum at casing, rotor diameters D=90 mm and d=85 mm.

5.0 CONCLUSIONS

On the basis of input parameters considered and results obtained, following conclusions are drawn in reference to the power output from air turbine-

- *The shaft power output at different casing and rotor diameters when vane angle is 36°, injection angle 22.5°, follows the decreasing trend from larger casing and rotor diameters to lower one, at injection pressure from 2-6 bars and speed of rotation 500 - 2500 rpm.*
- *The shaft power output at different casing and rotor diameters, when its difference (D-d) is kept constant, decreases linearly with respect to larger casing and rotor diameters to lower one, at injection pressure from 2 - 6 bars (30-90 psi).*
- *The optimum shaft power output is achieved at (D, d) = (90, 85) mm casing and rotor diameters respectively, at injection angle 22.5°, vane angle 36° (i.e.10 nos. vanes), when injection pressure is applied from 2-6 bars (30- 90 psi).*

REFERENCES

[1] Hubbert M. King, 1956, Nuclear energy and the fossil fuels; Amer. Petrol. Inst. Drilling and Production Practice, Proc. Spring Meeting, San Antonio, Texas. pp 7-25.

[2] Aleklett K., and Campbell C.J., 2003, The Peak and Decline of World Oil and Gas Production, Minerals and Energy - Raw Materials Report, Volume 18, Number 1, 2003, pp. 5-20.

[3] Singh B.R., and Singh, O., 2007, Use of Non-Conventional Energy for Sustainability to Fossil Fuel-National Conference on Recent Trend on Mechanical Engineering (RAME-2007), held on March, 28-29th , at Baba Sahab Dr. Bhim Rao Ambedkar College of Agricultural Engg. and Technology, Etawah-Proceedings pp 130-136.

[4] Singh B.R., and Singh, O., 2007, Uses of Wind Power as a Non-Conventional / Renewable Energy for Sustainability-National Conference on State of Art Technology in Mechanical Engineering (STEM-2007), held on October 29-31, 2007 at College of Technology,G.B. Pant University, Pant Nagar, UP-Proceedings pp 503-515.

[5] Honton E. J., 2004, Hydrogen Fuel Cell Car, presented at 15th Annual US Conference and Hydrogen Expo, April'2004, USA.

[6] Rose Robert, William J. Vincent, 2004, Fuel Cell Vehicle World Survey 2003, Breakthrough Technologies Institute, February' 2004, Washington, D.C.

[7] Singh B.R., and Singh O., 2006, Necessity and Potential for Bio-Diesel Use in India, Proceedings of International Conference on Bio-Fuel Vision-2015, October'13th -15th, 2006 at Bikaner, India Page 71-89.

[8] Singh, B.R., and Singh O., 2006, Study of Compressed Air as an alternative to fossil fuel for Automobile Engines, International Conference on Challenges and Strategies for Sustainable Energy and Environment- held on June 10-11th , at UPTU, Lucknow, UP-Proceedings pp 179-191.

[9] Singh B.R., and Singh, O., 2008, A Study on Sustainable Energy Sources and its Conversion Systems towards Development of an Efficient Zero Pollution Novel Turbine to be Used as Prime-mover to the Light Vehicle - 2008 ASME International Mechanical Engineering Congress and Exposition (IMECE-2008), on October 31-November 6, at Boston, Massachusetts, USA- Paper No. IMECE -2008 -66803.

[10] Singh B.R., and Singh O., 2008, Development of a vaned type novel Air Turbine, Proc. IMechE Vol. 222 Part C: J. Mechanical Engineering Science (The manuscript was received on December, 21st, 2007 and accepted for publication on 03rd June 2008) pp 2419-2426.

[11] Negre, Guy and Negre Cyril, 2004, Compressed Air - The Most Sustainable Energy Carrier for Community Vehicles, Speech in front of assembly at Kultur gathered for Fuel Cells World, Tuesday 29th June '2004.

[12] Saint Hilaire, G., Saint Hilaire, R., and Saint Hilaire, Y., 2005**,** Quasiturbine zero pollution car using gasoline, Festival at Le Lundi, Montreal Gazette, 26 September 2005**.**

[13] Knowlen C., Bruckner A. P., Mattick A.T., and Hertzberg A., 1998, Society of Automotive Engineers, Inc., High Efficiency Energy Conversion Systems for Liquid Nitrogen Automobiles, AIAA 98-1898.

[14] Fuglsang P., Bak C., Gunna M., 2004, Design and verification of the Ris0-B1 Airfoil-family for Wind Turbines, Journal of Solar Energy Engg., ASME Tran., Nov'2004, Vol.126 pp 1002-1008.

[15] Gorla, R., and Reddy, S., 2005, Probabilistic Heat Transfer and Structural Analysis of Turbine Blade, IJTJE, Vol. 22, pp 1- 11.

[16] Selig Michel S., 2004, Wind Tunnel Aerodynamics Tests of Six Airfoils for use on Small Wind Turbines, Journal of Solar Energy Engg., ASME Tran., Nov'2004, Vol.126, pp 986-1000.

[17] Schreck S., and Robinson M., 2004, Tip Speed Ratio Influences on Rationally Augmented Boundary Layer Topology and Aerodynamic Force Generation, Journal of Solar Energy Engg., ASME Tran., Nov' 2004, Vol.126 pp1025-1033.

[18] Singh B.R., and Singh, O., 2008, Development of a Vaned Type Novel Air Turbine, 12th International Symposium on Transport Phenomena and Dynamics of Rotating Machinery (ISROMAC-12), held on February 17-22, at Pacific Center of Thermal-Fluids Engineering, Sheraton Mohana Surfrider Hotel Honolulu, Hawaii, Paper No. ISROMAC-12-20046.

[19] Singh B.R., and Singh O., 2008, Energy Storage System to meet Challenges of 21st Century-an Overview - All India Seminar on Energy Management in Perspective of Indian Scenario, held on October 17-19, at Institution of Engineer (India), State Centre, Engineer's Bhawan, Lucknow, Proceedings Chapter15, pp 157-167.

[20] Singh B.R., and Singh, O.,2008, A Study to Optimize the Output of Vaned Type Novel Air Turbine, 4th International Conference on Energy Research and Development (ICERD-4), held on November,17-19, at State of Kuwait, Kuwait, Paper No. ICERD - 4 -1353.

[21] Singh, B.R., and Singh, O., 2008, A Study on Sustainable Energy Sources and its Conversion Systems towards Development of an Efficient Zero Pollution Novel Turbine to be used as Prime-mover to the Light Vehicle, 2008 ASME International Mechanical Engineering Congress and Exposition - held on October 31-November 6, at Boston, Massachusetts, USA, Paper No. IMECE - 2008 -66803.

[22] Singh, B.R., and Singh, O., 2008, Parametric Evaluation of Vane Angle on performance of Novel Air Turbine, Journal of Science, Engineering and Management**,** SITM, December, 2008, Vol. 2, pp 7-18.